Processing and Application of Ceramics 12 [2] (2018) 171–179
https://doi.org/10.2298/PAC1802171S

Influence of calcium doping on microstructure, dielectric and electric properties of $BaBi_2Nb_2O_9$ ceramics

Diana Szalbot, Małgorzata Adamczyk*, Beata Wodecka-Duś, Jolanta Dzik, Michał Rerak, Kamil Feliksik

Institute of Technology and Mechatronics, University of Silesia, 12, Żytnia St., 41-200 Sosnowiec, Poland

Received 30 October 2017; Received in revised form 6 March 2018; Received in revised form 17 May 2018; Accepted 7 June 2018

Abstract

Barium bismuth niobiate ($BaBi_2Nb_2O_9$) ceramics modified by calcium were prepared by solid state synthesis and two-step sintering process. An impact of calcium substitution on the A site of perovskite block is presented. The investigations are focused on dielectric as well as electric aspects of the modification. The presented results reveal that the concentration of a space charge is not preserved, what is surprising due to the homovalent nature of the dopant and no reason for creating additional lattice defects and charges connected. However, not only the valence of ions, but also the calcium-oxygen and barium–oxygen bond strength should be taken into consideration. Since the calcium–oxygen bond is probably weaker the loss of the bismuth oxide is expected to increase with an increase in the calcium content. Such a scenario results in appearance of a large number of negative charge carriers connected with unsaturated oxygen ions.

Keywords: *relaxor ferroelectric, lead-free materials, Aurivillius type materials, dielectric properties*

I. Introduction

Relaxor ferroelectric materials with classical perovskite structure constitute an interesting group of materials. They have been studied extensively not only due to their wide use in the electronic devices (multilayer ceramic capacitors, electrostrictive actuators, electromechanical transducers), but also due to the mechanism responsible for the features characteristic for relaxor behaviour. Over the past few decades a number of theoretical models have been developed to try to describe their properties. Their basic assumption is existence of polar nanoregions (PNRs), which provide unique physical properties [1–3]. Although the presence of PNRs in ferroelectric relaxors is noticed without a doubt, the mechanism and reasons for their formation have been the subject of discussion for several decades.

Bismuth-layered compounds, which consist of alternating bismuth oxide and perovskite type layers (the Aurivillius structure), are the next group of materials exhibiting the features characteristic for relaxor ferroelectrics. The most popular representative of this group is the compound $BaBi_2Nb_2O_9$ (BBN) widely investigated by many authors [4–6]. The $(Bi_2O_2)^{2+}$ layers are generally known to have a significant influence on the dielectric and electric conductivity properties of the Aurivillius structure [7]. In recent years the modification of BBN ceramics by incorporation of different cations on B and A sites of perovskite blocks as well as on bismuth oxide layers have been described in numerous reports in literature. The interest of authors was focused on changes in dielectric and relaxor properties [7–9].

In the present paper we discuss the impact of calcium substitution on A site of perovskite blocks. Our investigations did not focus only on the dielectric, but also on the electric aspect of the modification. Calcium could be heterovalent additive as well as homovalent. It depends on the manner of a replacement. Namely, Ca^{2+} ions could replace Ba^{2+} and in such situation they are homovalent admixture. The calcium ions could also incorporate into the bismuth-oxygen layers $(Bi_2O_2)^{2+}$ in the place of Bi^{3+} ions and behave as heterovalent modifier. Taking into consideration the value of ionic radii (Ca - 136 pm [10], Ba - 160 pm [10] and Bi - 96 pm [11])

*Corresponding author: tel: +48 32 3689242,
e-mail: *malgorzata.adamczyk-habrajska@us.edu.pl*

the first scenario is more likely to happen. The incorporation of homovalent admixture should keep the level of space charge concentration unchanged, although, the results presented in this article contradict this assumption. The reason for this will be discussed further in the paper.

II. Materials and characterization methods

The precursor powders ($BaBi_2Nb_2O_9$ with 0, 1 and 5 at.% of calcium) were prepared by solid state synthesis. The stoichiometric quantities of $BaCO_3$, Bi_2O_3 and Nb_2O_3 were weighed, homogenized and calcined at 950 °C for 2 h. The obtained powders were crushed, milled, sieved and then pressed into cylindrical pellets. The two-step sintering process was applied to all ceramic pellets. The first step at 950 °C for 2 h was used to form a layered perovskite phase at a relatively low temperature. The second step of sintering was used to prepare ceramic materials with well-formed microstructure. The samples were sintered in the closed crucibles at T_s = 1100 °C for the base BBN ceramics and at T_s = 1150 °C for the calcium modified ones. The sintering time was 6 h. The higher sintering temperature was selected due to the poor quality of the calcium modified BBN ceramics sintered at 1100 °C.

The phase purity and crystal structure were examined using XRD measurements which were carried out on powdered samples using a Huber diffractometer with monochromatic CuKα1 radiation (30 kV, 30 mA). The angle scale of the received diffraction diagrams was scaled to 2θ (Bragg-Brentano geometry) by Au standard (JCPDS number 12-0403). The diagrams were measured from 20 to 100° in 2θ with 0.05° steps. The grain structure and distribution of all elements throughout the grains were examined by scanning electron microscope (SEM, JSM-7100F TTL LV). The measurements were performed on the fractured surface of the sintered ceramics. The samples with surface area of 70 mm^2 and thickness of 0.6 mm were cut and polished for dielectric and impedance spectroscopy (IS) measurements. Subsequently, the gold electrodes were deposited on them by cathode sputtering. After that the samples were rejuvenated by thermal treatment at 450 °C to allow recombination and relaxation of a part of the frozen defects, formed during the sintering process. The dielectric data as well as impedance were measured using an HP 4192A impedance analyser in the 20 Hz–2 MHz frequency range and 300–823 K temperature range. The coherence of the obtained data was performed by K-K validation test [12,13]. Data fitting was performed using the ZView equivalent circuit software produced by Scribner Associates, USA. In order to perform the measurements of thermally stimulated depolarization currents (TSDC) the sample was first polarized in DC electric field with strength of 6 kV/cm, at 373 K for 10 min and then during subsequent cooling to temperature 300 K in the same field. Next, the sample was heated with a rate of 5 K/min throughout the diffused ferro-paraelectric phase transition up to 700 K. The TSDC were recorded numerically as a function of temperature and time during heating.

III. Results and discussion

3.1. Structural characterization

The X-ray diffraction patterns (XRD) of the BBN ceramics with 0, 1 and 5 at.% of calcium content obtained at room temperature are shown in Figure 1. The XRD profiles were analysed with the usage of DHN Powder Diffraction System ver. 2.3. The location and intensity of 32 diffraction lines were identified in the range of the measured angle. The obtained results show a good agreement with JCPDS standard number 12-0403 for $BaBi_2Nb_2O_9$. All line indexes connected with the Aurivillius structure were assigned. The appearance of a single, very weak, line was recorded on the diffraction pattern for the pure BBN ceramics. The origin of the line was widely discussed in our previous paper [6]. The pure and calcium doped ceramics are characterized by a tetragonal structure with space group $I4/mmm$ [14,15]. The lattice parameters obtained from X-ray patterns are presented in Table 1.

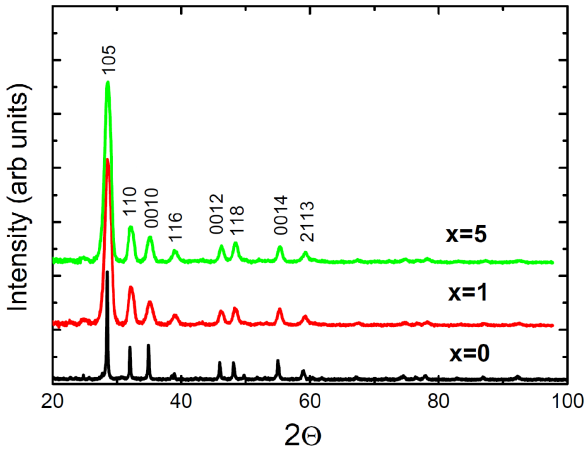

Figure 1. XRD patterns of BBN ceramics with calcium content of 0, 1 and 5 at.%

Table 1. The unit lattice parameters of calcium doped $BaBi_2Nb_2O_9$ ceramics

Ca-content [at.%]	0	1	5
a [Å]	3.941(3)	3.938(5)	3.936(6)
c [Å]	25.641(21)	25.622(71)	25.611(51)

Typical scanning electron images of the pure BBN and calcium doped ceramics are presented in the Fig. 2. The microstructure of the pure BBN ceramics consists of tile-shaped grains with rounded corners with various sizes, however small grains predominate. The average grain size is approximately 2 μm. In the case of the calcium doped ceramics the amount of larger grains increases, but the shape of the grain remains unchanged.

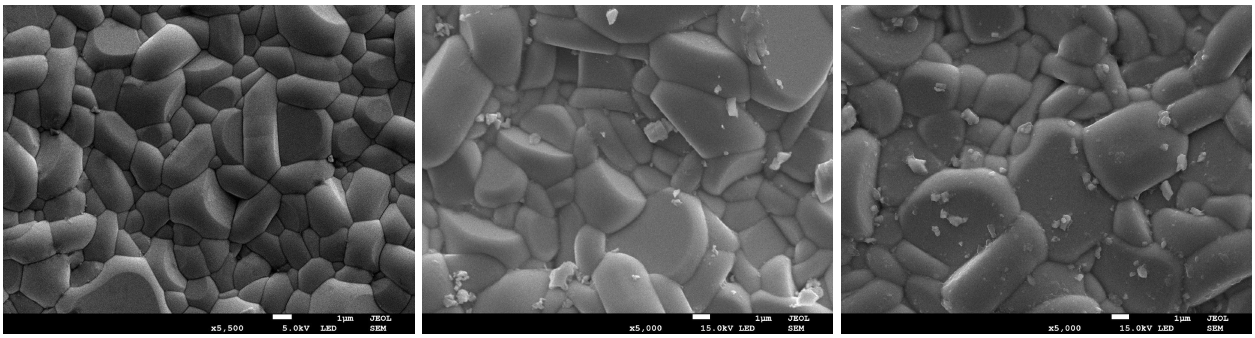

(a) (b) (c)

Figure 2. SEM pictures of $BaBi_2Nb_2O_9$ ceramics with: a) 0 at.%, b) 1 at.% and c) doped with 5 at.% Ca

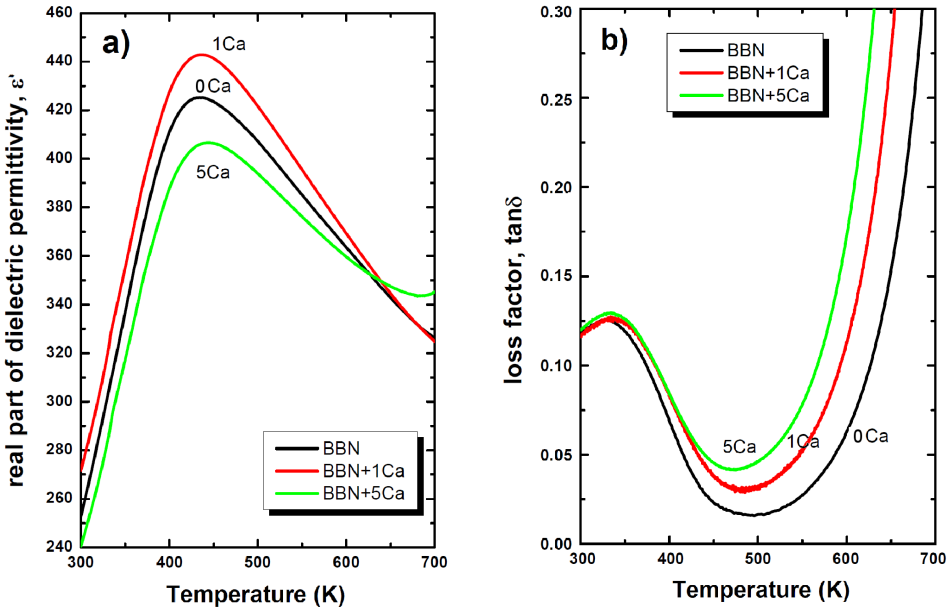

Figure 3. The real part of dielectric permittivity (a) and loss factor (b) as a function of the temperature, measured at frequency 10 kHz, for BBN ceramics with various Ca content

The increase in homogeneity of grain sizes corresponds to the increase in intergranular porosity and resulted in the decrease in relative density. The density of the unmodified ceramics, obtained by the Archimedes displacement method with distilled water, was 7.07 g/cm^3, whereas the density of the ceramics modified with 5 at.% of calcium was 6.94 g/cm^3. The changes of the morphology and grain size may not solely be an effect of doping, but also the difference in the sintering temperature (the pure BBN ceramics were sintered at 1100 °C, whereas the calcium modified ones at 1150 °C). Previously reported results [16] for the pure BBN ceramics indicated that the sintering temperature has a significant influence on the microstructure. The increase in sintering temperature leads to the grain growth. Thus, the average grain size changes from 2 to 4.5 μm when sintering temperature is increased from 1100 to 1120 °C. The average grain size of the ceramics modified by 1 at.% of calcium is approximately 2.5 μm, whereas the addition of 5 at.% of Ca caused increase in the average grain size up to 2.9 μm. After a comparison of the presently discussed results with the results described in the previous paper [16], the conclusion may be that the observed increase in the grain size is due to the admixture concentration increase and the temperature changes.

3.2. *Dielectric properties*

The temperature characteristics of dielectric permittivity ($\varepsilon(T)$) measured at frequency of 10 kHz is shown in Fig. 3. Presented temperature characteristic of the real part of dielectric permittivity (ε') shows diffused maximum at temperature T_m, which is shifted towards higher values and linearly dependent on the Ca content (Table 1). Moreover, calcium addition in the amount of 1 at.% resulted in a slight increase in the real part of dielectric permittivity (ε') in all investigated temperature ranges. Such behaviour is most likely related to the difference between the ionic radii of the dopant and the substituted Ba^{2+} ions. It should be mentioned that in normal perovskite the modification causes shrinkage in the dimensions of the unit cell. However, this may not be the case in the Aurivillius type structure, where the interslab lay-

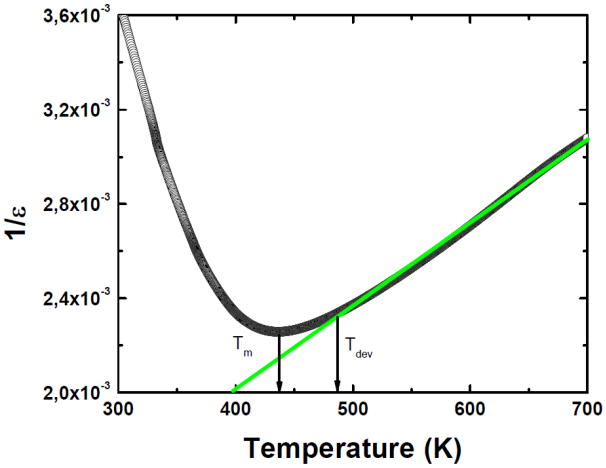

Figure 4. The temperature dependencies of inverse of dielectric permittivity ($1/\varepsilon$) for the $BaBi_2Nb_2O_9$ ceramics doped with 1 at.% Ca

ers can impose a constraint on the shrinkage, resulting in an enlarged rattling space for the cations in the octahedra [17,18] leading to the increase in the polarizability, which results in the increase in ε' value [19,20]. Furthermore, the increase of Ca-doping to 5 at.% results in a gradual decrease in ε'.

In classic ferroelectrics with sharp ferro-paraelectric phase transition the $1/\varepsilon(T)$ dependence follows the Curie-Weiss law in the high temperature range above the Curie temperature (T_c). However, the dependencies (Fig. 3) show a strong broadening of the dielectric permittivity maximum, so the reciprocal dielectric permittivity *vs.* temperature could be described by the Curie-Weiss law starting from temperature T_{dev} significantly higher than T_m (Fig. 4). The values of T_{dev} for ceramics containing 0, 1 and 5 at.% of calcium are equal to 459, 467 and 499 K, respectively.

In the temperature range between T_m and T_{dev} function $1/\varepsilon(T)$ could be described by the modified Curie-Weiss law, which allows to estimate the degree of diffuseness γ:

$$\frac{1}{\varepsilon'} - \frac{1}{\varepsilon'_{max}} = \frac{(T - T_{max})^{\gamma}}{C} \tag{1}$$

where ε'_{max} is the maximum value of dielectric permittivity at the transition temperature (T_m), C is the constant and γ is the degree of diffuseness. The limiting values 1 and 2 for γ reduce the expression to the Curie-Weiss law valid for the normal and quadratic dependence valid for the ideal relaxor ferroelectric. Figure 5 shows the plot of $\ln(1/\varepsilon - 1/\varepsilon'_{max})$ versus $\ln(T - T_c)$ for the doped BBN ceramics. The value of γ factor rapidly increases for the BBN with 1 at.% Ca, and gradually decreases for the ceramics with 5 at.% Ca.

The real part of dielectric permittivity obtained for all fabricated ceramic materials shows frequency dispersion characteristic for ferroelectric relaxors (Fig. 6). The maximum of ε' is reduced with the frequency increase and the corresponding temperature is shifted to a higher value. The degree of dispersion of ε'_{max}, defined as $\Delta\varepsilon'_{max} = \varepsilon_{max(100\,\mathrm{Hz})} - \varepsilon_{max(1\,\mathrm{MHz})}$, decreases considerably from 121 for the pure BBN ceramics to 65 for ceramics with 1 at.% of calcium, whereas the degree of dispersion of T_m ($\Delta T_m = T_{m(1\,\mathrm{MHz})} - T_{m(500\,\mathrm{Hz})}$) remains unchanged and it is 93 K.

It was found that the nonlinear dependence of $T_m(f)$ obeys to the Vogel-Fulcher relationship (Fig. 7):

$$f = f_0 \cdot \exp\left(\frac{-E_a}{k \cdot (T_m - T_f)}\right) \tag{2}$$

where E_a is the activation energy, T_f is the freezing temperature of polarisation fluctuation, and f_0 is the pre-exponential factor. It can be seen (Table 2) that the values of E_a, T_f and f_0, obtained from Eq. 2, depend on the calcium content. The freezing temperature T_f shifts to higher values and the value of E_a remains practically unchanged.

The changes in dielectric properties caused by the calcium modification are highly compatible with the results of TSDC measurements (Fig. 8). The results of

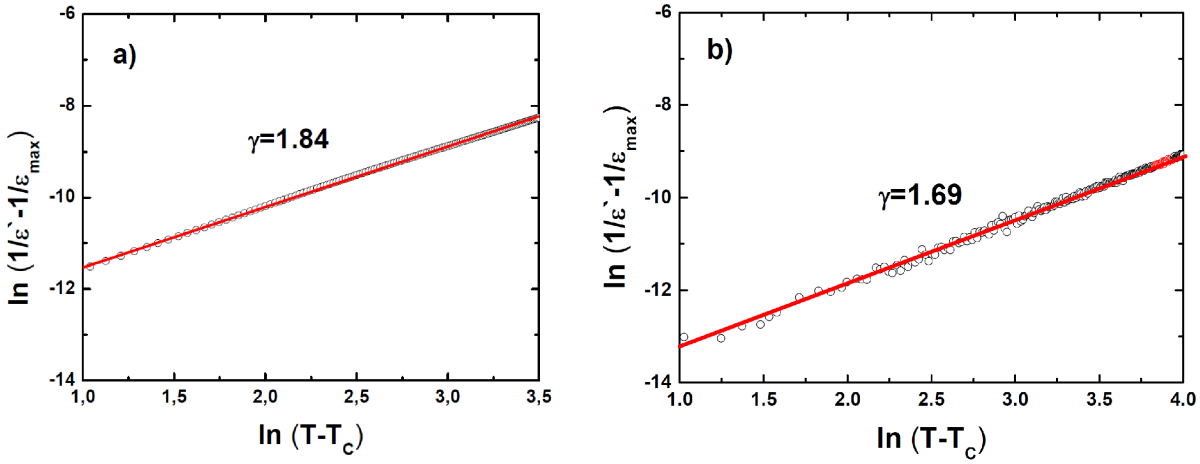

Figure 5. The plot of $\ln(1/\varepsilon - 1/\varepsilon_{max})$ as a function of $\ln(T - T_c)$ for the $BaBi_2Nb_2O_9$ ceramics doped with: a) 1 at.% Ca and b) 5 at.% Ca (solid red lines are the fit using Eq. 1)

Table 2. Transition temperature T_m, maximal dielectric permittivity at transition temperature ε_{max}, degree of diffusion γ, activation energy E_a, freezing temperature T_f and pre-exponential factor f_0

Ca-content [at.%]	$T_{m(100\,\mathrm{kHz})}$ [K]	$\varepsilon_{max(100\,\mathrm{kHz})}$	γ	E_a [eV]	T_f [K]	f_0 [Hz]
0	434.0	425.3	1.45	0.46	170	6.00×10^{13}
1	436.3	442.9	1.84	0.47	180	1.14×10^{13}
5	444.1	412.7	1.69	0.45	194	1.82×10^{13}

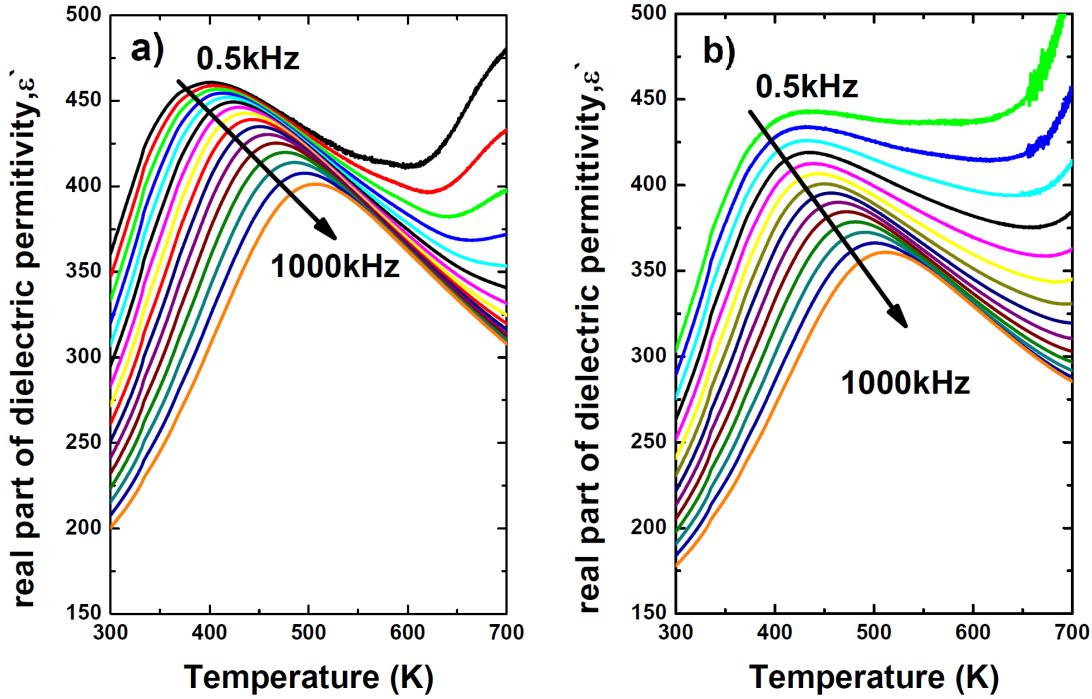

Figure 6. The real part of dielectric permittivity as a function of temperature measured on heating at various frequencies of measuring field, for BBN ceramics doped with: a) 1 at.% Ca and b) 5 at.% Ca

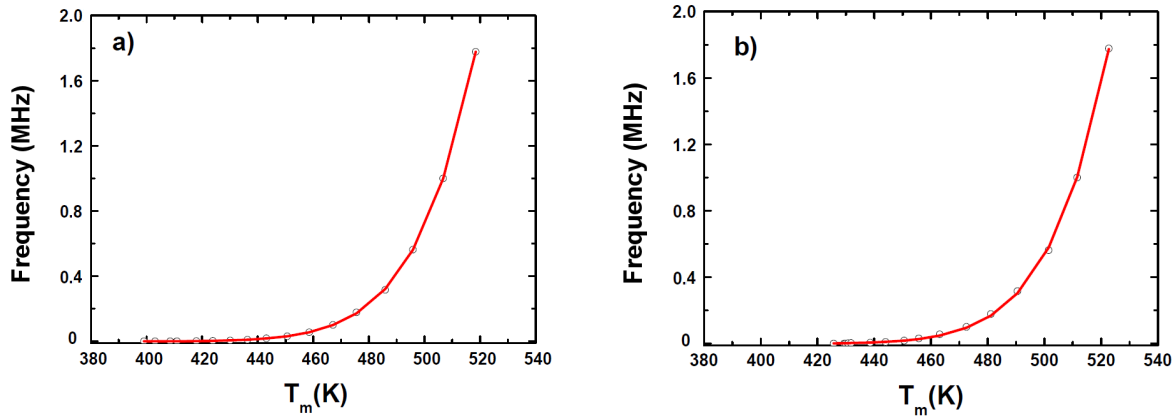

Figure 7. Measurement frequency as a function of temperature T_m for the $BaBi_2Nb_2O_9$ ceramics doped with: a) 1 at.% Ca and b) 5 at.% Ca (points are experimental data; the red lines are the fitting of the Vogel-Fulcher relationship)

TSDC measurements for the pure BBN ceramics were widely described in our previous paper [6]. For the pure BBN the temperature characteristic of TSDC reveals the highly broadened maximum appearing at temperatures higher than the temperature at which the ceramics were pre-polarized. The thermally stimulated depolarization currents are generally known to be inextricably connected with the presence of the space charge. The size of the discussed maximum indicates a high participation of the mentioned space charges in the ceramic materials. There is a question about the origin of these charges and we believe that they originate from the improper incorporation of barium. Namely, the ions only partly occupy the correct location in the perovskite blocks and a lot of barium ions incorporate into the $(Bi_2O_2)^{2+}$ layers in the places of bismuth vacancies or in the intermodal positions. Such behaviour of Ba^{2+} ions is associated with defects formation and plays a crucial role in

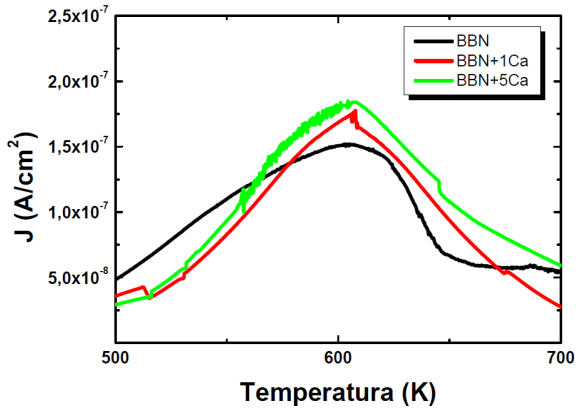

Figure 8. The thermally stimulated depolarization currents *vs.* temperature, for the undoped and Ca-modified BBN ceramics

the space charge formation. The addition of the calcium ions caused enlargement of TSDC maximum, which changes the maximal value of 1.5×10^{-7} A/cm^2 for the pure BBN, to 1.7×10^{-7} A/cm^2 for the BBN doped with 1 at.% Ca and 1.82×10^{-7} A/cm^2 for the sample with 5 at.% calcium. The results seem to be surprising and not easy to explain, because the cause of such behaviour is not obvious. As it has been mentioned above the calcium admixture is homovalent and the electrical balance is not disturbed. Thus, there is no reason for creating additional lattice defects and connected charges. The concentration of the space charge should be maintained. However both the valence of ions and barium–oxygen bond strength should be taken into consideration. Since the calcium–oxygen bond is probably weaker the loss of bismuth oxide is expected to increase with increase in the calcium content. Such scenario implies a large number of negative charge carriers connected with the unsaturated oxygen ions [21]. The assumption opened the way to the following investigations, in particular the detailed impedance spectroscopy.

3.3. *Impedance spectroscopy*

Figure 9 shows the frequency dependence of the real (Z') and imaginary (Z'') part of complex impedance at 500 °C for the pure and calcium modified ceramics. Incorporation of calcium into the BBN ceramics decreases the value of the real (Z') and imaginary (Z'') part of impedance. For all investigated ceramic materials plots of Z'' show broad peaks with maxima depending on the measurement temperature (Fig. 10). The maximum value of Z'' gradually decreases with the increases in frequency. Such behaviour suggests the existence of the thermally activated relaxation process connected with the presence of space charge polarization in the sample [22,23]. Moreover, the discussed maximum is not only broadened but also asymmetric, which indicates that the electrical processes occurred in the investigated ceramics are characterized by spread of relaxation time [24–26]. This is connected with the presence of immobile charges at low temperature and defects at higher ones [27,28]. The results confirm existence of the space charge in the samples and they are compatible with the TSDC measurements.

The Nyquist plots for all prepared ceramics suggest the decrease in the total resistivity (Fig. 11). The characteristic semicircle for the pure BBN ceramics has flattened shape with centre below the real axis [29]. Such a strong deformation was the reason for the choice of equivalent circuit with two parallel RC elements in series where the resistance of first is much lower than the second one (Fig. 12). The quality of such IS data description was not satisfactory, so the proposed circuit underwent insignificant modification – the capacitors were replaced by the constant phase element (CPE) [30,31]. The fitting procedure for the undoped BBN ceramics was widely described in our previously paper [29]. The obtained results allowed to determine the grain and grain boundary resistivity as well as the activation energy of electric conductivity phenomena taking place in both components of microstructure.

The characteristic semicircles for the calcium doped BBN ceramics (Fig. 11) also have a deformed shape, but the deformation is smaller. Such shape represents the grain effect in the ceramic materials [32]. The depression of the semicircle can be referred to the non-Debye type of relaxation correlated to several factors, such as

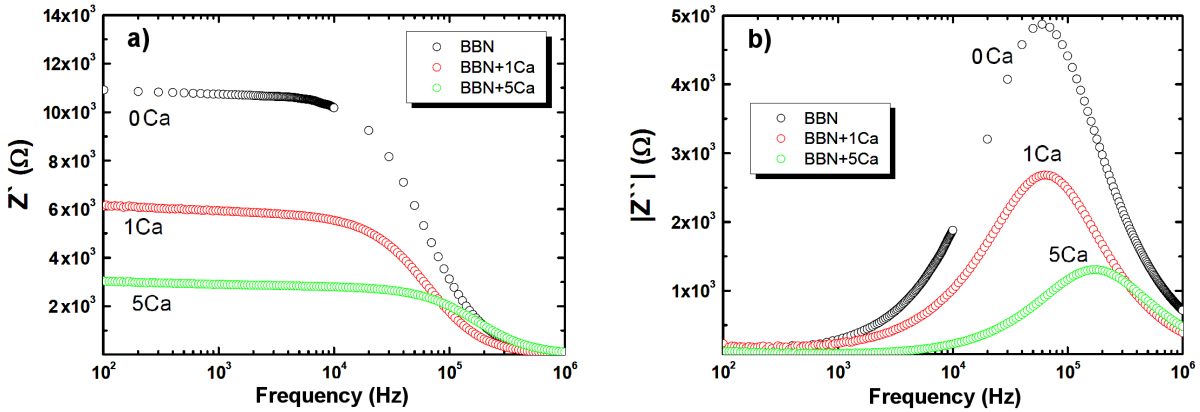

Figure 9. The frequency dependence of the real (a) and imaginary (b) part of the impedance at 773 K for $BaBi_2Nb_2O_9$ ceramics modified by calcium

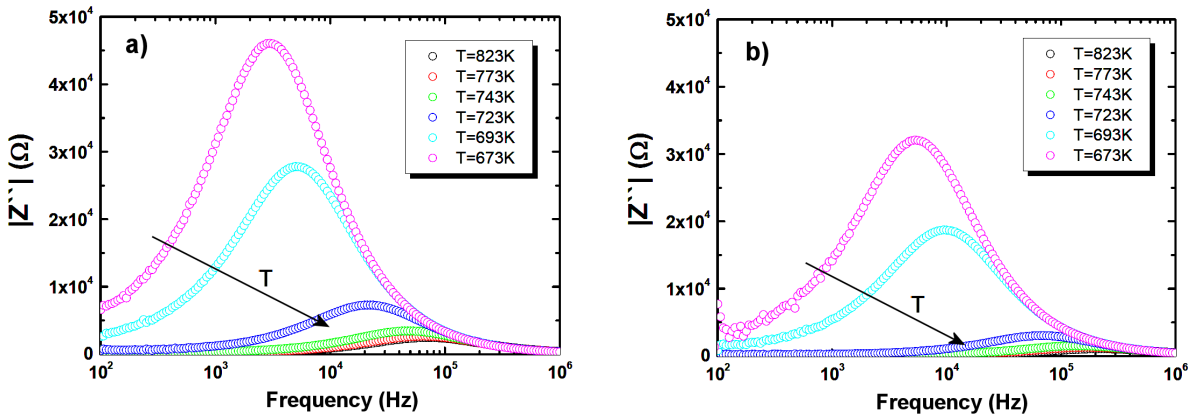

Figure 10. The frequency dependence of the real part of the impedance at various temperature for $BaBi_2Nb_2O_9$ ceramics modified by: a) 1 at.% Ca and b) 5 at.% Ca (the plots of Z'' *vs.* log$f$ for the pure BBN ceramics is available in our previous paper [29])

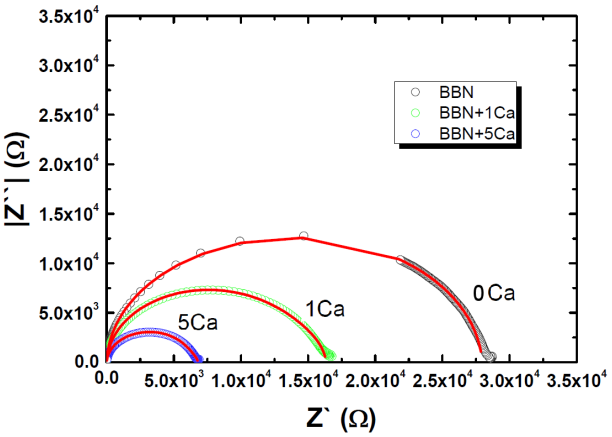

Figure 11. The experimental AC impedance spectrum in complex plane (open circles) and modelled impedance spectrum using calculated values of circuit elements (solid red line) for $BaBi_2Nb_2O_9$ ceramics with the different content of the calcium obtained at temperatures equal to 773 K

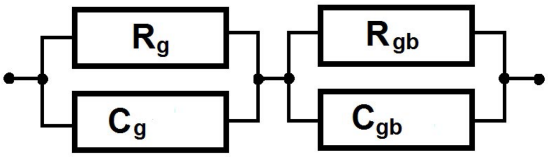

Figure 12. The equivalent circuit used to represent the impedance response of the pure and calcium modified BBN ceramics

grain boundaries, stress-strain phenomena, grain orientation and atomic defects distribution [32]. The grain resistance of the calcium doped ceramics was obtained by fitting the experimental results to the equivalent circuit containing one parallel CR elements. The grain resistivity for the calcium doped samples is smaller, but the calcium content dependences are not clear-cut (Fig. 13). The tendency is in good agreement with the results of TSDC measurements and it confirms the assumption about an influence of the calcium addition on the creation of oxygen vacancies. The additional number of negative charge carriers connected with unsaturated oxygen ions results in a decrease in sample resistivity. The diagrams of the natural logarithm of the obtained grain resistivity versus reciprocal of absolute temperature have a linear character. The slope of dependences significantly changes with the Ca content over the entire discussed temperature range, what is connected with the changes of the activation energy obtained from the Arrhenius formula:

$$R = R_0 \cdot \exp\left(-\frac{E_a}{k \cdot T}\right) \tag{3}$$

The directional coefficient of the linear equation enables to estimate the activation energy of grain conductivity for all of the discussed samples. The obtained results are presented in Table 3.

Table 3. Activation energy values calculated from impedance data for grain (E_G) resistivity

Ca-content [at.%]	E_G [eV]
0	1.00
1	0.84
5	0.91

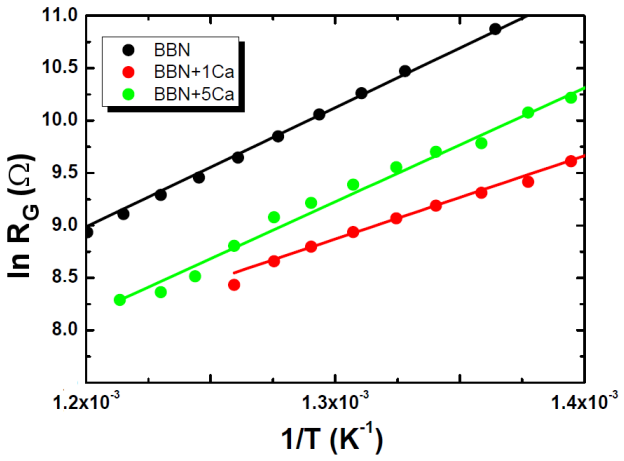

Figure 13. Arrhenius plots for calculation of conduction activation energies of grains

IV. Conclusions

The main purpose of the paper was to present the effect of the calcium doping on the microstructure, dielectric and electric properties of $BaBi_2Nb_2O_9$ ceramics. The discussed results reveal limiting role of the modifier in the formation of microstructure features such as a shape and a size of grains, whereas the influence of the calcium on the electric and dielectric properties was significant. Namely, the small amount of calcium (1 at.%) caused an increase in the dielectric permittivity in the whole investigated temperature range. The additional increase in Ca concentration changes this tendency. The value remains practically unchanged from room temperature up to 350 K and then the loss factor increases following the increase in the calcium content. The feature, combined with the specific behaviour of thermostimulated depolarization currents and impedance spectroscopy, signals the possibility of creation of additional oxygen vacancies.

References

1. V. Westphal, W. Kleeman, M.D. Glinchuk, "Diffuse phase transitions and random-field induced domain states of the "relaxor" ferroelectric $PbMg_{1/3}Nb_{2/3}O_3$", *Phys. Rev. Lett.*, **68** (1992) 847–850.
2. C. Stock R.J. Birgeneau, S. Wakimoto, G. Shirane "Universal static and dynamic properties of the structural transitions in $PbZn_{1/3}Nb_{2/3}O_3$", *Phys. Rev. B*, **69** (2004) 094104.
3. M.A. Helal, M. Aftabuzzaman, S. Tsukada, S. Kojima "Role of polar nanoregions with weak random fields in Pb-based perovskite ferroelectrics", *Sci. Report*, **7** (2017) 44448.
4. Y. Shimakawa, Y. Kubo, Y. Nakagawa, S. Goto, T. Kamiyama, H. Asano and F. Izumi, "Crystal structure and ferroelectric properties of $ABi_2Ta_2O_9$ (A = Ca, Sr, and Ba)", *Phys. Rev. B*, **61** (2000) 6559.
5. Ismunandar, B.J. Kennedy, Gunawan, Marsongkohadi, "Structure of $ABi_2Nb_2O_9$ (A = Sr, Ba): Refinement of powder neutron diffraction data", *J. Solid State Chem.*, **126** (1996) 135–141.
6. M. Adamczyk, Z. Ujma, M. Pawełczyk, "Dielectric properties of $BaBi_2Nb_2O_9$ ceramics", *J. Mater. Sci.*, **41** (2006) 5317–5322.
7. Y. Wu, Ch. Nguzen, S. Seraji, M. Forbess, S.J. Limmer, "Doping effect in layer structured $SrBi_2Nb_2O_9$ ferroelectrics", *J. Am. Ceram. Soc.*, **84** (2001) 2882–2888.
8. M.K. Adak, S.S. Mondal, D. Dhak, S. Sen, "Investigation of density of states and electrical properties of $Ba_{0.5}Co_{0.5}Bi_2Nb_2O_9$ nanoceramics prepared by chemical route", *J. Mater. Sci.: Mater. Electron.*, **28** [6] (2017) 4676–4683.
9. C. Karthik, K.B.R. Varma, "Influence of vanadium doping on the processing temperature and dielectric properties of barium bismuth niobate ceramics", *Mater. Sci. Eng. B*, **129** [1-3] (2006) 245–250.
10. Y. Wu, M.J. Forbess, S. Seraji, S.J. Steve, J. Limmer, T.P. Chou, C. Nguyen, G.Z. Cao, "Doping effect in layer structure $SrBi_2Nb_2O_9$ ferroelectrics", *J. Appl. Phys.*, **90** (2001) 5296–5302.
11. M.J. Forbess, S. Seraji, Y. Wu, C. Nguyen, G.Z. Cao, "Dielectric properties of layered perovskite $Sr_{1-x}A_xBi_2Nb_2O_9$ ferroelectrics (A = La, Ca and x = 0, 0.1)", *J. Appl. Phys.*, **76** (2000) 2934–2936.
12. B. Boukamp "A linear Kroning-Kramers transform test for immitance data validation", *J. Electrochem. Soc.*, **142** (1995) 1885–1894.
13. B. Boukamp "Electrochemical impedance spectroscopy in solid state ionic: Recent advances", *Solid State Ionics*, **169** (2004) 65–73.
14. S.M. Blake, M.J. Faconer, M. McCreedy, P. Lightfoot, "Cation disorder in ferroelectric Aurivillius phase of the type $Bi_2ANb_2O_9$ (A = Ba, Sr, Ca)", *J. Mater. Chem.*, **7** (1997) 1609–1613.
15. R. Macquart, B.J. Kennedy, T. Vogt, Ch.J. Howard, "Phase transition $BaBi_2Nb_2O_9$: Implications for layered ferroelectrics", *Phys. Rev. B*, **66** (2002) 212102.
16. M. Adamczyk, Z. Ujma, M. Pawełczyk, L. Szymczak, L. Kozielski, "Influence of sintering conditions on relaxor properties of $BaBi_2Nb_2O_9$ ceramics", *Phase Transitions*, **79** [6-7] (2006) 435–445.
17. H. Gu, J. Xue, J. Wang, "Significant dielectric enhancement in $0.3BiFeO_3$-$0.7SrBi_2Nb_2O_9$", *Appl. Phys. Lett.*, **79** (2001) 2061–2063.
18. K. Singh, D.K. Bopardikar, D.V. Atkare, "A compendium of Tc-Us and Ps-Δz data for displacive ferroelectrics", *Ferroelectrics*, **82** (1988) 55–67.
19. M. Adamczyk, L. Kozielski, M. Pawełczyk, M. Pilch, "Dielectric and mechanical properties of $BaBi_2(Nb_{0.99}V_{0.01})_2O_9$ ceramics", *Arch. Metall. Mater.*, **56** [4] (2011) 1163–1168.
20. M. Adamczyk, L. Kozielski, M. Pilch, M. Pawełczyk, A. Soszyński, "Influence of vanadium dopant on relaxor behaviour of $BaBi_2Nb_2O_9$ ceramics", *Ceram. Int.*, **39** [4] (2013) 4589–4595.
21. V. Shrivastava "Lattice strain dielectric insulation response of $Sr_{1-x}Ca_xBi_2Nb_2O_9$ ceramics", *J. Adv. Dielectrics*, **6** [3] (2016) 1650021.
22. S.R. Hasan, U. Prasad, N. Kumar, R. Ranjan, R.N.P. Choudhary, "Investigation of impedance and electric modulus properties of bismuth layer-structure compound barium bismuth niobate", *Intern. J. Latest Technol. Eng. Manag. Appl. Sci.*, **4** (2015) 51–54.
23. B.N. Parida, P.R. Das, R. Padhee, R.N.P. Choudhary "Phase transition and conduction mechanism of rare earth based tungsten-bronze compounds", *J. Alloys. Compd.*, **540** (2012) 267–274.
24. G. Goodman, *Ceramic materials for electronics*, R.C. Buchanan Marcel Dekker, New York, 1986.
25. C.K. Suman, K. Prasad, R.N.P. Choudhary, "Impedance spectroscopic studies of ferroelectric $Pb_2Sb_3DyTi_5O_{18}$ ceramic", *Adv. Appl. Ceram.*, **104** (2005) 294–299.
26. S. Sen, R.N.P. Choudhary, A. Tarafdar, P. Pramanik, "Impedance spectroscopy study of strontium modified lead zirconate titanate ceramics", *J. Appl. Phys.*, **99** (2006) 124114.
27. A.K. Jonascher, "The universal dielectric response", *Nature*, **267** (1977) 673–679.
28. D.P. Almond, A.R. West, "Impedance and modulus spectroscopy of "real" dispersive conductors", *Solid State Ionics*, **11** (1983) 57–64.
29. M. Adamczyk, L. Kozielski, M. Pilch, "Impedance spectroscopy of $BaBi_2Nb_2O_9$ ceramics", *Ferroelectrics*, **417**

[1] (2011) 1–8.
30. H. Jaffe, "Piezoelectric ceramics", *J. Am. Ceram. Soc.*, **41** (1958) 494–498.
31. H. Jaffe, D.A. Berlincourt, "Piezoelectric transducer materials", *Proc. IEEE*, **53** (1965) 1372–1386.
32. T. Badapanda, R.K. Harichandan, S.S. Nayak, A. Mishra, S. Anwar "Frequency and temperature dependence behaviour of impedance, modulus and conductivity of $BaBi_4Ti_4O_{15}$ Aurivillius ceramic", *Process. Appl. Ceram.*, **8** [3] (2014) 145–153.